Jordan Journal of Civil Engineering, Volume **12**, No. **2**, **2018**

Effect of Parabolic-Concave Thickness Variation on the Mechanical Buckling Resistance of Simply Supported FGM Plates

Ali Meksi [1], *Khalil Belakhdar* [2)*], *Otbi Bouguenina* [3], *Abdelouahed Tounsi* [4] *and El-Abbes Adda Bedia* [4]

[1] Department of Civil Engineering, University of Mustapha Stambouli, Mascara, 29000, Algeria.
[2] Department of Science and Technology, University Center of Tamanrasset, 11000, Algeria.
[*] Corresponding Author. E-Mail:be.khalil@gmail.com.
[3] Department of Science and Technology, University Center Nour Bachir of El-Bayadh, 32000, Algeria.
[4] Laboratory of Materials and Hydrology, University of Sidi Bel Abbes, 22000, Algeria.

ABSTRACT

A numerical investigation on the buckling resistance of FGM plates having parabolic-concave thickness variation exposed to in-plane loading is presented in this piece of research work. An analytical formulation is derived and the governing differential equation of stability is solved numerically using finite difference method. A specific function of thickness variation is introduced, where this function controls the parabolic variation intensity of the plate thickness without changing its original material volume. The results indicated that the loss ratio in the buckling resistance due to parabolic-concave thickness variation is highly dependent on the geometrical properties of the plate, while it is not affected by the material properties or by the distribution profile of the constituent materials. Influencing material and geometrical parameters on the degradation of the buckling resistance are investigated, which may help in design guidelines of such complex structures.

KEYWORDS: Buckling, Finite difference method, Parabolic-concave thickness variation, Numerical analysis.

INTRODUCTION

Functionally Graded Materials (FGMs) are considered as composites made of two or more constituent phases with smoothly varying properties through the thickness. Smoothness can be realized by gradually varying the volume fraction of the constituent materials. Usually, FGMs are composed of metal and ceramic, where the thermal protection system is assured by ceramic and the second (metal) has a high mechanical strength. Nowadays, (FGMs) are used in many engineering and industrial domains, like aircraft, space vehicles, high temperature thermal barriers, ... etc. For a particular application, the FGM system has the ability to resist thermal and mechanical loadings simultaneously.

Stability analysis of FGM plates under mechanical and/or thermal loading has been carried out by many researchers using different theories and solutions (Saha et al., 2012; Reddy et al., 2013; Bouazza et al., 2012 and 2013; Fekrar et al., 2013; Ramu Mohanty 2014). Various cases of loading and boundary conditions have been extensively studied for FGM plates with constant thickness. However, plates having variable thickness have also attracted the attention of designers and researchers. In general, geometrically complex FGM plates, such as variable thickness plates, have become common in different engineering and industrial fields

Received on 1/7/2017.
Accepted for Publication on 1/11/2017.

due to design requirements. In spite of that, pieces of research work conducted to study FGM plates with variable thickness are fewer in number compared to those conducted on constant thickness plates.

Generally, the analytical formulations for the analysis of geometrically complex structures, like plates with variable thickness, are characterized by their complexity. As an example, Mozafari et al. (2010, 2012) studied the stability of FGM plates with linearly varying thickness under mechanical buckling load. They presented a higher-order theory. They used Sanders non-linear strain-displacement and the weighted residual method to derive the buckling load.

Besides, some researchers utilized simple assumptions to ease the formulations when including thickness variation. Ait Atmane et al. (2011) presented a formulation based on Bernoulli-Euler beam theory to study the free vibration of sigmoid functionally graded beams with variable cross-section. Pouladvand (2009) examined thermal stability of thin FG rectangular plates with variable thickness based on classical plate theory. Based on high-order theory, Alinaghizadeh and Shariati (2016) evaluated the non-linear bending analysis of thick, two-directional FG annular sector plates with variable thickness and different boundary conditions resting on a non-linear elastic foundation.

On the other side, other researchers adopted numerical methods for the analysis of plates under different loading cases with the inclusion of variable thickness. Rajasekaran and Wilson (2013) presented a numerical solution using finite difference method to evaluate the exact buckling loads and vibration frequencies of variable thickness isotropic plates. Various combinations of boundary conditions as well as many types of loading were considered. Also, Bouguenina et al. (2015) proposed a numerical solution using finite difference method to investigate thermal buckling of simply supported FG plates with linearly variable thickness. Ghomshei and Abbasi (2013) developed a finite element formulation for analyzing the axisymmetric thermal buckling of FGM annular plates with variable thickness.

The main purpose of the present research work is to study the mechanical buckling resistance of FGM plates having parabolic-concave thickness variation. To attend this objective, the derived governing equation of stability is solved numerically by using the finite difference method in order to have the ability to include the thickness variation, noting that such task is complex to be performed analytically. A special parabolic-concave function is developed to control the intensity of the parabolic variation of the plate thickness, but without changing its original material volume. A parametric study is conducted to investigate the effect of different parameters on the critical buckling load.

THEORETICAL FORMULATION

Material Constitutive Relations

We consider a functionally graded plate, composed of a mixture of ceramic and metal. It is assumed that the composition properties of an FGM plate vary through the thickness of the plate according to a simple power-law function. The volume fractions of ceramic (V_c) and metal (V_m) are given as:

$$\begin{cases} V_c = \left(\frac{z}{h} + \frac{1}{2}\right)^k \quad ; \quad -\frac{h}{2} \le z \le \frac{h}{2} \\ V_m(z) + V_c(z) = 1 \end{cases} \tag{1}$$

k is a parameter that controls the material variation profile, where $0 \le k \le \infty$.

The modulus (E) is expressed assuming that the Poisson's ratio is constant ($\nu = 0.3$).

$$E(z) = E_c V_c + E_m(1 - V_c) \tag{2}$$

Formulation of Stability Equations

The displacements of the neutral plane of the FGM plate in the $(x, y \text{ and } z)$ directions are denoted u, v and w, respectively. (ϕ_x) and (ϕ_y) denote the rotations of the mid-plate normal about (x) and (y) axes. Based on the first-order shear deformation theory, the strains are given as:

$$\begin{cases}\varepsilon_x = u_{,x} + z\phi_{x,x} \\ \varepsilon_y = \mathrm{v}_{,y} + z\phi_{y,y} \\ \gamma_{xy} = u_{,y} + \mathrm{v}_{,x} + z(\phi_{x,y} + \phi_{y,x}) \\ \gamma_{xz} = \phi_x + w_{,x} \\ \gamma_{zy} = \phi_y + w_{,y}\end{cases} \quad (3)$$

The stress-strain relationships according to Hook's law are:

$$\begin{cases}\sigma_x = \frac{E}{1-\nu^2}(\varepsilon_x + \nu\varepsilon_y) \\ \sigma_y = \frac{E}{1-\nu^2}(\varepsilon_y + \nu\varepsilon_x) \\ \sigma_{xy} = \frac{E}{2(1+\nu)}\gamma_{xy} \ ; \ \sigma_{xz} = \frac{E}{2(1+\nu)}\gamma_{xz}; \\ \sigma_{zy} = \frac{E}{2(1+\nu)}\gamma_{zy}\end{cases} \quad (4)$$

The forces and moments per unit length are given in terms of the stress components through the thickness as:

$$\begin{cases}N_i = \int_{-h/2}^{h/2}\sigma_i dz \quad ; \ i = x, y, xy \\ M_i = \int_{-h/2}^{h/2}\sigma_i z dz \ ; i = x, y, xy \\ Q_i = \int_{-h/2}^{h/2}\sigma_{iz} dz \quad ; \ i = x, y\end{cases} \quad (5)$$

Substituting Eqs. (2) to (4) into Eq. (5) yields:

$$\begin{cases}N_x = \frac{E_1}{1-\nu^2}(u_{,x} + \nu\mathrm{v}_{,y}) + \frac{E_2}{1-\nu^2}(\phi_{x,x} + \nu\phi_{y,y}) \\ N_y = \frac{E_1}{1-\nu^2}(\nu u_{,x} + \mathrm{v}_{,y}) + \frac{E_2}{1-\nu^2}(\nu\phi_{x,x} + \phi_{y,y}) \\ N_{xy} = \frac{E_1}{2(1+\nu)}(u_{,y} + \mathrm{v}_{,x}) + \frac{E_2}{2(1+\nu)}(\phi_{x,y} + \phi_{y,x}) \\ M_x = \frac{E_2}{1-\nu^2}(u_{,x} + \nu\mathrm{v}_{,y}) + \frac{E_3}{1-\nu^2}(\phi_{x,x} + \nu\phi_{y,y}) \\ M_y = \frac{E_2}{1-\nu^2}(\nu u_{,x} + \mathrm{v}_{,y}) + \frac{E_3}{1-\nu^2}(\nu\phi_{x,x} + \phi_{y,y}) \\ M_{xy} = \frac{E_2}{2(1+\nu)}(u_{,y} + \mathrm{v}_{,x}) + \frac{E_3}{2(1+\nu)}(\phi_{x,y} + \phi_{y,x}) \\ Q_x = \frac{E_1}{2(1+\nu)}(\phi_x + w_{,x}) \\ Q_y = \frac{E_1}{2(1+\nu)}(\phi_y + w_{,y})\end{cases} \quad (6)$$

where

$$(E_1, E_2, E_3) = \int_{-h/2}^{h/2}(1, z, z^2)E(z)dz \quad (7)$$

The equations of equilibrium are given according to Von Karman's tensor by:

$$\begin{cases}N_{x,x} + N_{xy,y} = 0 \\ N_{y,y} + N_{xy,x} = 0 \\ M_{x,x} + M_{xy,y} - Q_x = 0 \\ M_{xy,x} + M_{y,y} - Q_y = 0 \\ (Q_{x,x} + Q_{y,y} + q + N_x w_{,xx} + N_y w_{,yy} + 2\,N_{xy} w_{,xy}) = 0\end{cases} \quad (8)$$

By eliminating the variables (u, v, ϕ_x, ϕ_y) through manipulating Eqs. (6) and (8), we get:

$$\nabla^4 w + D_1\nabla^2(N_x w_{,xx} + N_y w_{,yy} + 2\,N_{xy} w_{,xy} + q) + D_2(N_x w_{,xx} + N_y w_{,yy} + 2\,N_{xy} w_{,xy} + q) = 0 \quad (9)$$

$$\begin{cases}D_1 = \frac{2(1+\nu)}{E_1} \\ D_2 = -\frac{E_1(1-\nu^2)}{E_1 E_3 - E_2^2}\end{cases} \quad (10)$$

The critical equilibrium method is used to establish the stability equations. So, by assuming that the state of stable equilibrium of a general plate under in-plane load may be designated by the deflection (w_0), the displacement of the neighboring state is given by:

$$\Delta w = w_0 + w_1 \quad (11)$$

where w_1 is an arbitrarily small increment of displacement. Substituting Eq. (11) into Eq. (9) and re-evaluating the original equation result in the following stability equation:

$$\nabla^4 w_1 + D_1\nabla^2(N_x^0 w_{1,xx} + N_y^0 w_{1,yy} + 2\,N_{xy}^0 w_{1,xy}) + D_2(N_x^0 w_{1,xx} + N_y^0 w_{1,yy} + 2\,N_{xy}^0 w_{1,xy}) = 0 \quad (12)$$

where (N_x^0, N_y^0) and (N_{xy}^0) are the resulting pre-buckling forces.

By considering a square plate subjected to in-plane loads, the pre-buckling forces can be obtained by using the equilibrium conditions as:

$$\begin{cases}N_x^0 = \xi_1 P \\ N_y^0 = \xi_2 P \\ N_{xy}^0 = 0\end{cases} \quad (13)$$

where (P) is the force per unit length, (ξ_1) and (ξ_2)

are the load parameters that indicate the loading conditions, noting that negative values for (ξ_1) and (ξ_2) correspond to compressive loadings.

Substituting Eq. (13) into Eq. (12), we obtain:

$$\nabla^4 w_1 + \mathrm{D}_1 P \nabla^2 \left(\xi_1 w_{1,xx} + \xi_2 w_{1,yy}\right) + D_2 P \left(\xi_1 w_{1,xx} + \xi_2 w_{1,yy}\right) = 0 \quad (14)$$

FINITE DIFFERENCE SOLUTION

The fourth-order differential relationship presented by Eq. (14) can be solved numerically using finite difference method. To do that, we consider a rectangular FGM plate meshed into $(n \times m)$ nodes spaced by (Δ) in (x) and (y) directions, as shown in Figure 1.

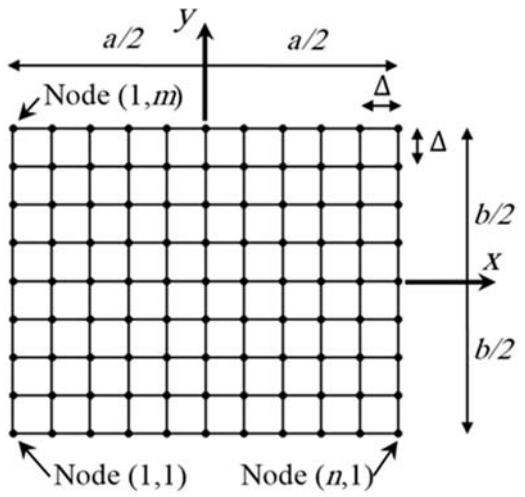

Figure (1): Finite difference mesh of the plate

The governing relationship given by Eq. (14) is written in finite difference format (mesh) as:

$$\left(10(2 + (\xi_1 + \xi_2)C_1 P)\right) w_{1_{(i,j)}} + (2 + D_1(\xi_1 + \xi_2)P)\left(w_{1_{(i+1,j+1)}} + w_{1_{(i+1,j-1)}} + w_{1_{(i-1,j-1)}} + w_{1_{(i-1,j+1)}}\right) + (C_2 P - 8)\left(w_{1_{(i+1,j)}} + w_{1_{(i-1,j)}}\right) + (C_3 P - 8)\left(w_{1_{(i,j+1)}} + w_{1_{(i,j-1)}}\right) + (D_1 P\, \xi_1 + 1)\left(w_{1_{(i+2,j)}} + w_{1_{(i-2,j)}} + w_{1_{(i,j+2)}} + w_{1_{(i,j-2)}}\right) = 0 \quad (15)$$

where

$$\begin{cases} C_1 = D_1 - D_2\, \Delta^2/5 \\ C_2 = D_1(-6\,\xi_1 - 2\,\xi_2) + D_2\, \Delta^2 \xi_1 \\ C_3 = D_1(-2\,\xi_1 - 6\,\xi_2) + D_2\, \Delta^2 \xi_2 \end{cases} \quad (16)$$

This mesh is applied at nodes with coordinates $(i = 2..n-1, j = 2..m-1)$, noting that this operation will result in virtual nodes along the lines $(i = 2, i = n-1,\ j = 2, j = m-1)$.

Since the plate is simply supported, the boundary conditions are given as follows:

$$\begin{cases} \text{at } x = 0, a: & w_1 = 0; \quad M_{x1} = 0; \quad \phi_y = 0 \\ \text{at } y = 0, b: & w_1 = 0; \quad M_{y1} = 0; \quad \phi_x = 0 \end{cases} \quad (17)$$

The null displacements along the edges are expressed as:

$$w_{1_{(i,j)}} = 0 \text{ at } \begin{cases} i = (1, n),\ j = (1..m) \\ i = (1..n),\ j = (1, m) \end{cases} \quad (18)$$

By expressing the null moments along the edges in terms of the deflection w_1, the virtual nodes are simply eliminated resulting in a system of $(n-2) \times (m-2)$ simultaneous equations expressed as:

$$[A]\{w_1\} = \{0\} \quad (19)$$

Evaluation of P_{cr}

The simultaneous relationships represented by Eq. (19) cannot be solved, because the matrix $[A]$ contains the unknown force (P). This problem is solved by using the trial and error technique as follows:

- Step (1): In the first trial, an initial value equal to unity is assigned to (P),
- Step (2): After solving the system of Eq. (19), the first mode shape $\left(w_1^{(1)}\right)$ is used to calculate the critical buckling load (P_{cr_1}) using Eq. (14), as follows:

$$P_{cr} = -\frac{\nabla^4 w_1^{(1)}}{D_1 \nabla^2 \left(\xi_1 w_{1,xx}^{(1)} + \xi_2 w_{1,yy}^{(1)}\right) + D_2 P \left(\xi_1 w_{1,xx}^{(1)} + \xi_2 w_{1,yy}^{(1)}\right)} \quad (20)$$

It is worth noting that the following equation is calculated numerically using its finite difference format as follows:

$$P_{cr} = -\frac{\begin{pmatrix} 20w_{1(i,j)} - 8\left(w_{1(i+1,j)} + w_{1(i-1,j)} + w_{1(i,j+1)} + w_{1(i,j-1)}\right) + 2\left(w_{1(i+1,j+1)} + w_{1(i+1,j-1)} + w_{1(i-1,j+1)} + w_{1(i-1,j-1)}\right) + \\ w_{1(i+2,j)} + w_{1(i-2,j)} + w_{1(i,j+2)} + w_{1(i,j-2)} \end{pmatrix}}{\begin{pmatrix} 10C_1(\xi_1+\xi_2)w_{1(i,j)} + D_1(\xi_1+\xi_2)\left(w_{1(i+1,j+1)} + w_{1(i+1,j-1)} + w_{1(i-1,j+1)} + w_{1(i-1,j-1)}\right) + D_1\xi_1\left(w_{1(i+2,j)} + w_{1(i-2,j)}\right) + \\ D_1\xi_2\left(w_{1(i,j-2)} + w_{1(i,j+2)}\right) + C_2\left(w_{1(i+1,j)} + w_{1(i-1,j)}\right) + C_3\left(w_{1(i,j+1)} + w_{1(i,j-1)}\right) \end{pmatrix}} \quad (21)$$

- Step (3): The obtained (P_{cr_1}) is used for another iteration to solve the simultaneous Eq. (19), where a new critical buckling load (P_{cr_2}) is obtained.
- Step (2) and (3) are repeated successively until the solution is converged and the following criterion is violated:

$$\frac{P_{cr_i} - P_{cr_{i-1}}}{P_{cr_i}} \leq 10^{-5} \quad (22)$$

VALIDATION OF FINITE DIFFERENCE METHOD

In order to validate the present numerical method, the predicted critical buckling loads for simply supported FG plates are compared with those in the literature. Assumed is an FGM plate consisting of aluminum and alumina, where the Young's modulus of alumina is $E_c = 380\ GPa$ and of aluminum is $E_m = 70GPa$. Poisson's ratio is assumed to be constant for both metal and ceramic with a value of $\nu = 0.3$.

Table 1 summarizes the critical buckling for a simply supported square plate under different in-plane load cases, for different values of the material distribution parameter k and aspect ratio (a/b). The results in Table 1 are given for different mesh sizes $(a/\Delta = 10, 20, 30, 40)$ to test the convergence of the finite difference solution. Additionally, to enhance the accuracy of the predicted results, Richardson's extrapolation formula is adopted, which is expressed as given by Eq. (23) (Szilard, 2004).

$$P_{cr}^{[ex]} = P_{cr}^{[40]} + \frac{P_{cr}^{[40]} - P_{cr}^{[20]}}{2^{\mu}-1} \quad (23)$$

where $P_{cr}^{[ex]}$ is the extrapolated value, $\left(P_{cr}^{[20]}\right)$ and $\left(P_{cr}^{[40]}\right)$ are the values of critical buckling load obtained by using mesh size $a/\Delta = 20$ and mesh size $a/\Delta = 40$, respectively. $\mu = 2$ is the exponent value, which depends on the convergence characteristics of the numerical method.

By comparing the present results against those reported in previously published works (Bouazza, 2012 and 2013; Mohammadi, 2009), it can be observed that the results are in excellent agreement, which validates the present numerical method.

FGM PLATE WITH PARABOLIC THICKNESS VARIATION

As mentioned previously, the objective of this study deals with investigating the buckling resistance of simply supported FGM plates with parabolic thickness variation. The proposed function changes only the intensity of the parabolic thickness variation, while it conserves the original material volume of the plate. Two types of thickness variation have been studied; parabolic variation in one direction and parabolic variation in both directions, as shown in Figure 2.

In case of one direction, the plate thickness becomes a function of x which is derived according to the following general parabolic function:

$$H(x) = -\frac{4}{a^2}(e_0 - e_1)x^2 + e_0 \quad (24)$$

where e_0 is the thickness at the plate mid center $(x = 0)$ and (e_1) is the thickness at the plate edges; i.e., at $x = (-a/2\ , a/2)$.

Table 1. Comparison between present numerical method and exact solutions of P_{cr}(MN/m)

k	Ref.	Mesh size $a/\Delta h$	(ξ_1,ξ_2)= (-1,0)			(ξ_1,ξ_2) =(0,-1)			(ξ_1,ξ_2)= (-1,-1)		
			***a/b*=0.5**	***a/b*=1**	***a/b*=1.5**	***a/b*=0.5**	***a/b*=1**	***a/b*=1.5**	***a/b*=0.5**	***a/b*=1**	***a/b*=1.5**
k=0	Present	10	2.1317	1.3619	1.5957	8.4744	1.3619	0.7125	1.7033	0.6809	0.4925
		20	2.1409	1.3703	1.6077	8.5506	1.3703	0.7154	1.7122	0.6852	0.4951
		30	2.1426	1.3719	1.6100	8.5647	1.3719	0.7159	1.7139	0.6859	0.4955
		40	2.1432	1.3724	1.6107	8.5697	1.3724	0.7161	1.7145	0.6862	0.4957
		∞ ($P_{cr}^{[ex]}$)	**2.1440**	**1.3731**	**1.6117**	**8.5761**	**1.3731**	**0.7163**	**1.7153**	**0.6865**	**0.4959**
	Bouazza(2013)		2.1440	1.3732	1.6118	8.5761	1.3732	0.7163	1.7152	0.6866	0.4959
	Bouazza(2012)		2.1466	1.3738	1.6123	8.5862	1.3738	0.7166	1.7172	0.6869	0.4961
	Mohammadi(2009)		2.1466	1.3738	1.4907	8.5862	1.3738	0.7166	1.7172	0.6869	0.4961
k=1	Present	10	1.0627	0.6789	0.7954	4.2248	0.6789	0.3551	0.8491	0.3394	0.2455
		20	1.0673	0.6831	0.8014	4.2627	0.6831	0.3566	0.8536	0.3415	0.2468
		30	1.0682	0.6839	0.8025	4.2698	0.6839	0.3569	0.8544	0.3419	0.2470
		40	1.0685	0.6841	0.8029	4.2723	0.6841	0.3569	0.8547	0.3421	0.2471
		∞ ($P_{cr}^{[ex]}$)	**1.0689**	**0.6844**	**0.8034**	**4.2755**	**0.6844**	**0.3570**	**0.8551**	**0.3423**	**0.2472**
	Bouazza(2013)		1.0689	0.6845	0.8034	4.2755	0.6845	0.3571	0.8551	0.3422	0.2472
	Bouazza(2012)		1.0699	0.6848	0.8036	4.2797	0.6848	0.3572	0.8559	0.3424	0.2473
	Mohammadi(2009)		1.0699	0.6848	0.7430	4.2797	0.6848	0.3572	0.8559	0.3424	0.2473
k=2	Present	10	0.8293	0.5297	0.6207	3.2966	0.5297	0.2771	0.6626	0.2649	0.1916
		20	0.8328	0.5330	0.6253	3.3263	0.5330	0.2782	0.6661	0.2665	0.1926
		30	0.8335	0.5336	0.6262	3.3318	0.5336	0.2785	0.6667	0.2668	0.1927
		40	0.8337	0.5338	0.6265	3.3337	0.5338	0.2785	0.6669	0.2669	0.1928
		∞ ($P_{cr}^{[ex]}$)	**0.8340**	**0.5341**	**0.6269**	**3.3362**	**0.5341**	**0.2786**	**0.6672**	**0.2670**	**0.1929**
	Bouazza(2013)		0.8341	0.5341	0.6269	3.3362	0.5341	0.2786	0.6672	0.2671	0.1929
	Bouazza(2012)		0.8349	0.5343	0.6271	3.3395	0.5343	0.2787	0.6679	0.2672	0.1930
	Mohammadi(2009)		0.8349	0.5343	0.5798	3.3395	0.5343	0.2787	0.6679	0.2672	0.1930

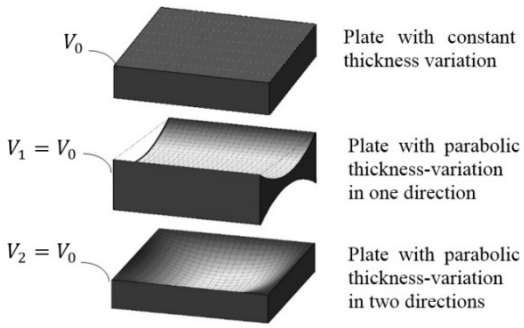

Figure (2): Parabolic thickness variation profiles

Let (V_0) be the volume of constant thickness plate (original plate) which has a constant thickness (h) and let (V_1) be the volume of variable-thickness plate, where:

$$V_0 = a.b.h \tag{25}$$

$$V_1 = a.b\left(\frac{2}{3}(e_0 - e_1) + e_1\right) \tag{26}$$

By maintaining the same volumes of both plates as $V_0 = V_1$, we get:

$$e_1 + 2e_0 = 3h \tag{27}$$

Expressing e_0 in terms of (e_1) as:

$$e_1 = \eta.e_0 \tag{28}$$

where η represents the plate edge-to-mid center thickness ratio and noting that $\eta > 1$ corresponds to parabolic-concave variation.

Substituting Eq. (27) and Eq. (28) into Eq. (24), we obtain the thickness variation function as:

$$H(x) = \frac{3h}{2+\eta}\left(\frac{4(\eta-1)}{a^2}x^2 + 1\right) \tag{29}$$

Thus, the thickness variation function is expressed by one parameter η that controls the intensity of the parabolic variation and keeps the volume of the new plate equal to that of the original plate, as shown in Figure 3.

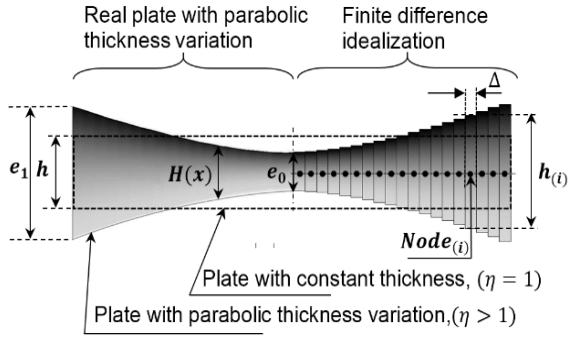

Figure (3): Finite difference idealization of FGM plate with parabolic thickness variation

In case of plate having variable thickness in two directions, the thickness function is derived from the following general parabolic equation:

$$H(x,y) = \frac{16(e_0-e1)}{a^2b^2}x^2y^2 - \frac{4(e_0-e1)}{a^2}x^2 - \frac{4(e_0-e1)}{b^2}y^2 + e_0 \quad (30)$$

Let (V_2) be the volume of this plate, which is given as follows:

$$\mathrm{V_2} = \mathrm{a.b}\left(\frac{4}{9}(\mathrm{e_0} - \mathrm{e_1}) + \mathrm{e_1}\right) \quad (31)$$

By making $V_0 = V_2$, we get:

$$5e_1 + 4e_0 = 9h \quad (32)$$

Expressing (e_0) in terms of (e_1) as:

$$e_1 = \eta . e_0 \quad (33)$$

Substituting Eq. (32) and Eq. (33) into Eq. (30), the function $H(x,y)$ can be written as follows:

$$H(x,y) = \frac{9h}{4+5\eta}\left(4(\eta-1)\left(\frac{x^2}{a^2}+\frac{y^2}{b^2}-4\frac{x^2y^2}{a^2b^2}\right)+1\right) \quad (34)$$

Similarly, the intensity parameter η controls the intensity of the parabolic variation in the two directions and keeps the volume of the new plate equal to that of the original constant-thickness plate as clarified in Figure 3.

Finite Difference Considerations

In the finite difference idealization in case of variable-thickness plate, it is assumed that at each discrete $(Node_{(i,j)})$, the thickness is constant given by $(h_{(i,j)})$ as shown in Figure 3. The value of $(h_{(i,j)})$ is simply calculated by substituting the node's coordinates in the thickness function $H(x)$ or $H(x,y)$ given by Eq. (29) or Eq. (34). In this case, the coordinate $(z_{(i,j)})$ at each $(Node_{(i,j)})$ varies in its specific domain: $\left[-\frac{h_{(i,j)}}{2}, \frac{h_{(i,j)}}{2}\right]$. Based on Eq. (1), the material distribution profile through the thickness will be the same at each node, since the volume fractions of the material constituents are dependent on the ratio z/h; i.e.,$z_{(i,j)}/h_{(i,j)} = [-1,+1]$.

Based on that, all the equations containing the thickness parameter h, such as Eq. (7), are calculated by using the constant value $(h_{(i,j)})$. In addition, the integration expressions through the thickness are evaluated using the trapezoidal rule, noting that each thickness $(h_{(i,j)})$ is divided into 2000 subdivisions.

RESULTS AND DISCUSSION

The effect of the parabolic variation intensity parameter η (edge-to-mid thickness ratio) on the critical buckling load of simply supported FGM square plates with side to thickness ratio $a/h = 50$ exposed to different cases of loading, is shown in Figures 4 to 6.

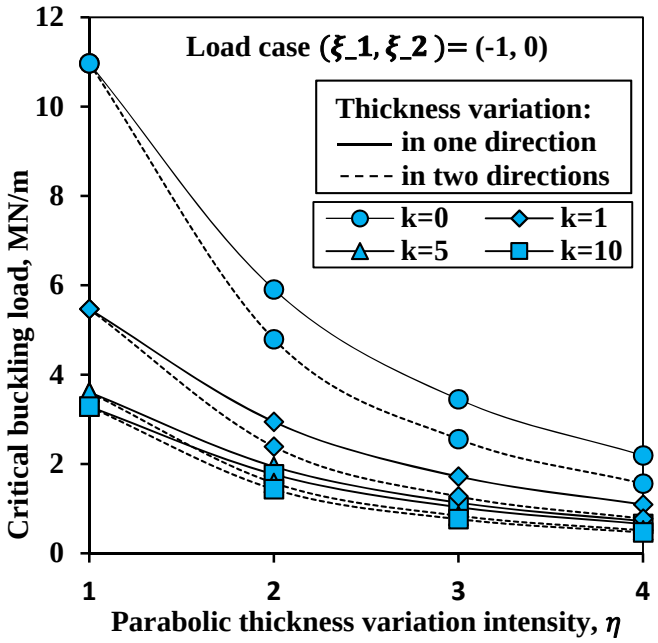

Figure (4): Effect of parabolic variation intensity parameter η on critical buckling temperature of FGM plate with $a/h=50$, exposed to x-uniaxial in-plane load

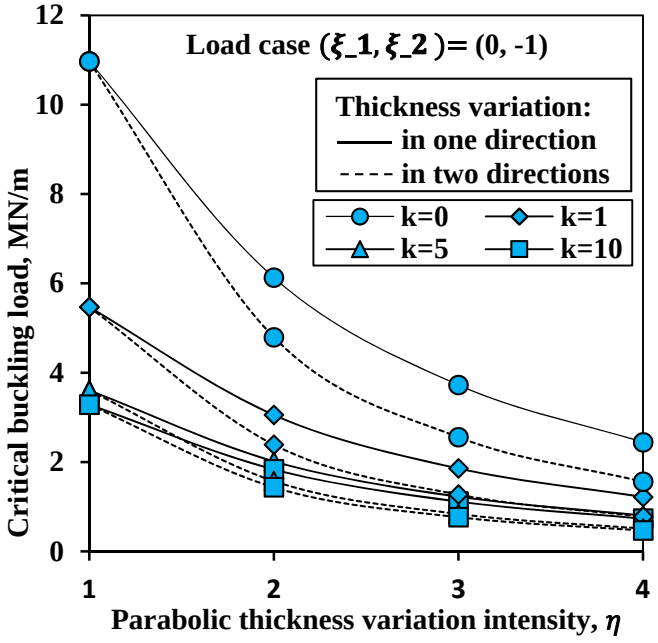

Figure (5): Effect of parabolic variation intensity parameter η on critical buckling temperature of FGM plate with $a/h=50$, exposed to y-uniaxial in-plane load

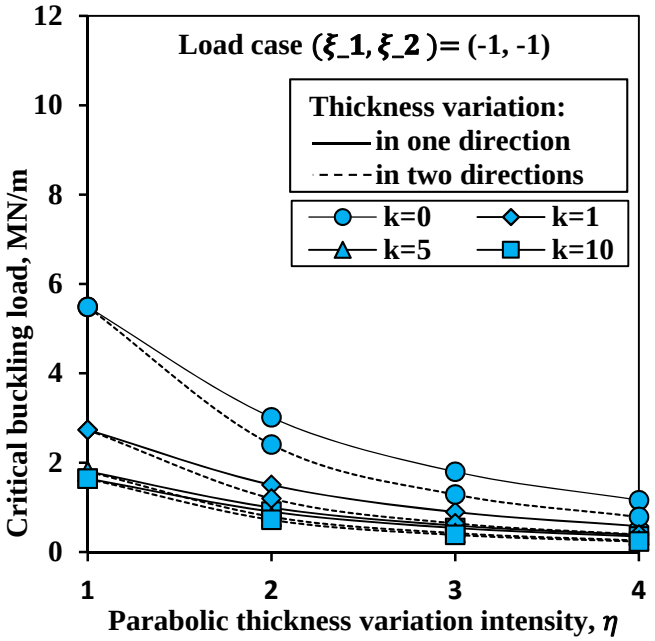

Figure (6): Effect of parabolic variation intensity parameter η on critical buckling temperature of FGM plate with *a/h=50*, exposed to biaxial in-plane load

The general note that can be observed from these figurers is that varying the thickness geometry of the plate to fit a parabolic-concave shape decreases significantly its buckling resistance, especially when the thickness variation is applied in two directions. In addition, the critical buckling load of an FGM plate having parabolic thickness variation is affected by the material distribution profile, where as the value of the power law index k increases, the critical buckling load decreases. This is because plates with high metal content have lower stiffness compared to ones with high ceramic content.

Figure 7 represents the loss ratio of buckling resistance in FGM plates with parabolic thickness variation in terms of parabolic variation intensity η. The loss ratio meant here is the loss ratio of the buckling resistance; the degradation ratio of the critical buckling load of FGM plate with variable thickness ($\eta > 1$) with respect to that of the original constant plate thickness ($\eta = 1$). The loss ratio is simply calculated as follows:

$$\text{The loss ratio in } P_{cr} = \left(\frac{P_{cr\left(\substack{\text{constant}\\\text{thickness}}\right)} - P_{cr\left(\substack{\text{variable}\\\text{thickness}}\right)}}{P_{cr\left(\substack{\text{constant}\\\text{thickness}}\right)}} \right) \quad (35)$$

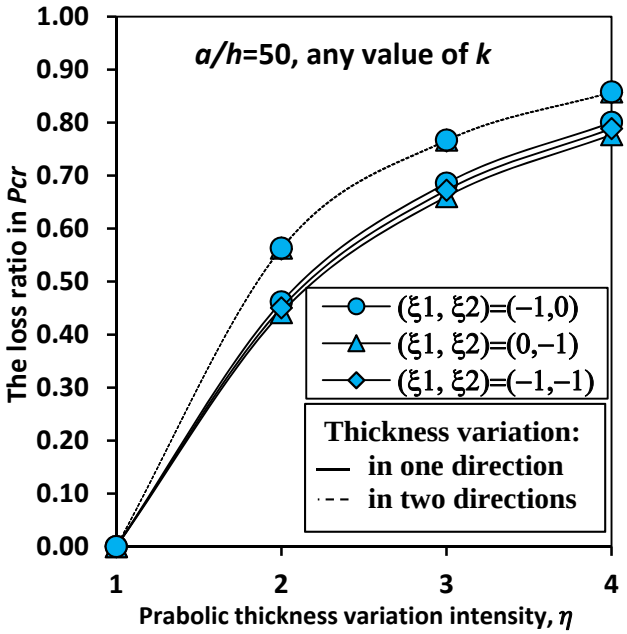

Figure (7): Loss ratio in buckling resistance of FGM plate with parabolic thickness variation in terms of η

Based on Figure 7, the results indicate that the loss ratio in the critical buckling load increases as the parameter η increases. This is justified by the fact that the increase in the value of (η) helps the occurrence of buckling, since it reduces the thickness at the plate-middle, where the buckling starts to develop. Also, it is noticed that the relationship between the loss ratio of the buckling resistance and the parabolic variation intensity (η) is not affected by the variation of the volume fraction of the constituent materials (k), which means that whatever the value of k is, the loss ratio in the critical buckling load is the same. Here, it can be concluded that the loss ratio in the critical buckling load is the same in a homogenous plate and an FGM plate if they have the same geometric properties, including the parabolic thickness variation dimensions.

Moreover, when the thickness variation is applied in two directions, the loss ratio in the buckling resistance under uniaxial in-plane load is almost the same as under biaxial load. However, when the thickness variation is applied in one direction, the predicted loss ratios in the buckling resistance for each loading case in terms of (η) are close to each other.

The variation of the loss ratio in the critical buckling load of simply supported square FGM plates having parabolic thickness variation in one direction and in two directions in terms of the side-to-thickness ratio (a/h), is presented in Figure 8 and Figure 9, respectively.

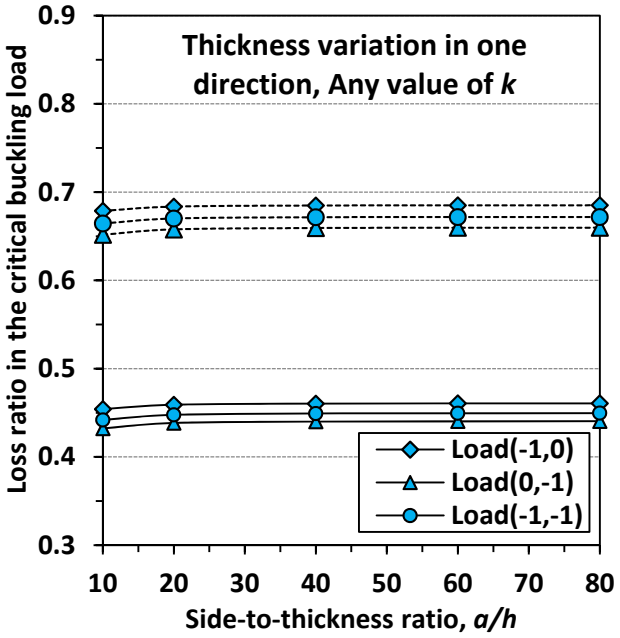

Figure (8): Effect of side-to-thickness ratio *a/h* on the loss ratio in the buckling resistance of FGM plate with thickness variation in one direction

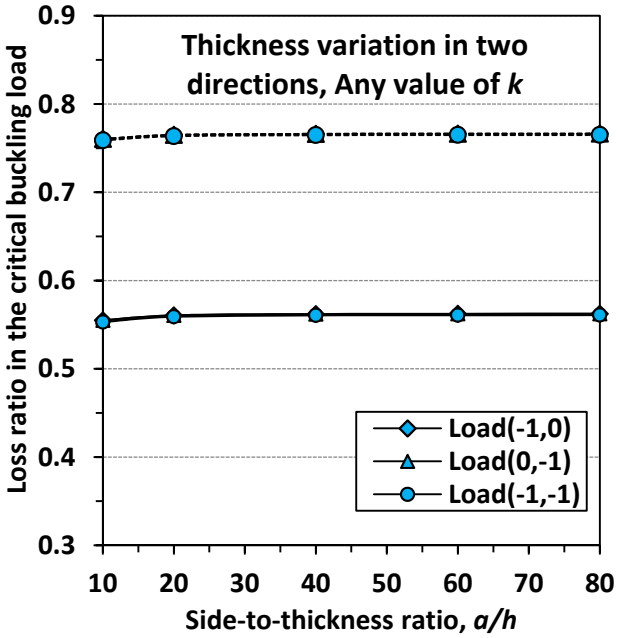

Figure (9): Effect of side-to-thickness ratio *a/h* on the loss ratio in the buckling resistance of FGM plate with thickness variation in two directions

Generally, in Figures 8 and 9, it is shown that the loss ratio in the buckling resistance is highly affected by the thickness variation intensity parameter η, while it is slightly affected by the load case or the side-to-thickness ratio. The results also indicated that the material profile index k has a negligible effect on the loss ratio of the buckling resistance of FGM plates.

The results indicated that the loss ratio in the buckling resistance equals about 45% and 0.65% for η equal to 2 and 3, respectively, in case of applying the thickness variation in one direction. However, when applying the thickness variation in two directions, the buckling resistance of the plate is reduced to 75% and 0.56% for thickness variation intensity η equal to 2 and 3, respectively. According to what was found in Figure 7, it is concluded that when applying parabolic-concave thickness variation to plates having the same geometric properties, they will lose the same buckling resistance independently from material properties and distribution profile. Additionally, when the parabolic thickness variation is applied in two directions, the in-plane loading case (uniaxial, biaxial) will have a small effect on the loss ratio of the buckling resistance of the plate.

CONCLUSIONS

In the present research work, the mechanical stability of simply supported FGM plates is investigated in order to study the degradation in the buckling resistance after varying the plate thickness according a parabolic-concave function. The governing equation is solved numerically using finite difference method to have the ability to include the thickness variation. Effects of different geometrical and material properties on the buckling resistance of FGM plates are studied.

The results obtained indicated that applying parabolic thickness variation to simply supported FGM plates with preserving their original material volume leads to the following main conclusions:

– Parabolic thickness variation intensity reduces significantly the critical buckling load of the plate, especially when the variation is applied in the two

longitudinal directions.

- The loss ratio in the buckling resistance of plates is highly dependent on the geometrical properties of the plate thickness (i.e., parabolic intensity variation), but it is slightly sensible to material properties and distribution profiles.
- When parabolic thickness variation is applied in two directions, the in-plane loading case (uniaxial, biaxial) has a small effect on the loss ratio of the buckling resistance of the plate.

REFERENCES

Ait Atmane, H., Tounsi, A., Ziane, N., and Mechab, I. (2011). "Mathematical solution for free vibration of sigmoid functionally graded beams with varying cross-section". Steel Comp. Struct., 11 (6), 489-504.

Alinaghizadeh, F., and Shariati, M. (2016). "Geometrically non-linear bending analysis of thick two-directional functionally graded annular sector and rectangular plates with variable thickness resting on non-linear elastic foundation". Comp. Part B: Eng., 86, 61-83.

Bouazza, M., Hammadi, F., Seddiki, S., and Adda-Bedia, E.A. (2013). "Mechanical stability of moderately thick functionally graded plates". J. of Frontiers in Constr. Eng., 2 (3), 60-65.

Bouazza, M., Ouinas, D., Yazid, A., and Hamouine, A. (2012). "Buckling of thin plates under uniaxial and biaxial compression". J. of Mat. Sci. and Eng., 2 (8), 487-492.

Bouguenina, O., Belakhdar, K., Tounsi, A., and Adda, B. (2015). "Numerical analysis of FGM plates with variable thickness subjected to thermal buckling". Steel Comp. Struct., 19 (3), 679-695.

Fekrar, A., Zidi, M., Boumia, L., Ait Atmane, H., Tounsi, A., and Bedia Adda, E.A. (2013). "Thermal buckling of Al/Al_2O_3 functionally graded plates based on first-order theory". Nature and Tech., A (08), 12-16.

Ghomshei, M.M., and Abbasi, V. (2013). "Thermal buckling analysis of annular FGM plate having variable thickness under thermal load of arbitrary distribution by finite element method". J. of Mech. Sci. and Tech., 27 (4), 1031-1039.

Mohammadi, M., Saidi, A.R., and Jomehzadeh, E. (2009). "Levy solution for buckling analysis of functionally graded rectangular plates". Appl. Compos. Mater., 17 (1), 81-93.

Mozafari, H., Ayob, A., and Alias, A. (2010). "Influence of thickness variation on the buckling load in plates made of functionally graded materials". Eur. J. Sci. Res., 47 (3), 422-435.

Mozafari, H., and Ayob, A. (2012). "Effect of thickness variation on the mechanical buckling load in plates made of functionally graded materials". Procedia Tech., 1, 496-504.

Pouladvand, M. (2009). "Thermal stability of thin rectangular plates with variable thickness made of functionally graded materials". J. Solid Mech., 1 (3), 171-189.

Rajasekaran, S., and Wilson, A.J. (2013), "Buckling and vibration of rectangular plates of variable thickness with different end conditions by finite difference technique". Str. Eng. and Mech., 46 (2), 269-294.

Ramu, I., and Mohanty, S.C. (2014). "Buckling analysis of rectangular functionally graded material plates under uniaxial and biaxial compression load". Procedia Eng., 86, 748-757.

Reddy, B.S., Kumar, J.S., Reddy, C.E., and Reddy, K. (2013). "Buckling analysis of functionally graded material plates using higher-order shear deformation theory". J. of Comp., 1-12.

Rohit, S., and Maiti, P.R. (2012), "Buckling of simply supported FGM plates under uniaxial load". Int. J. of Civil and Str. Eng., 2 (4), 1035-1050.

Szilard, R. (2004). "Theories and applications of plate analysis: classical numerical and engineering methods". John Wiley and Sons.